

# Silicon isotope composition of dissolved silica in surface waters of the Elbe Estuary and its tidal marshes

Andreas Weiss · Christina De La Rocha ·  
Thorben Amann · Jens Hartmann

Received: 17 September 2014 / Accepted: 12 February 2015 / Published online: 8 March 2015  
© Springer International Publishing Switzerland 2015

**Abstract** Land ocean silica fluxes pass estuaries. Recent data suggest that the isotopic composition of dissolved silica (DSi) is not altered during this transition. This could have major implication for the oceanic isotopic silicon cycle. To improve our knowledge about isotopic Si cycling in estuaries we investigate the silicon isotopic composition ( $\delta^{30}\text{Si}$ ) of DSi of the Elbe Estuary and for the first time of tidal marsh areas. DSi concentrations in the tidal marshes were generally higher during seepage phase than during bulk phase. Negligible tidal variation in  $\delta^{30}\text{Si}$  ( $1.71 \pm 0.08$ – $1.87 \pm 0.13$  ‰) occurred in the freshwater marsh. In the brackish marsh  $\delta^{30}\text{Si}$  was higher during the seepage phase than during the bulk phase, with highest noted values being  $>2.78 \pm 0.11$  ‰. In

the salt marsh, seepage water had lower  $\delta^{30}\text{Si}$  than bulk water over a total range of  $1.81 \pm 0.03$ – $2.62 \pm 0.02$  ‰. In the estuary in October, DSi concentrations in the freshwater zone were diminished through removal by diatoms. The  $\delta^{30}\text{Si}$  of DSi increased from  $1.43 \pm 0.11$  to  $2.33 \pm 0.08$  ‰. In December, DSi concentrations increased along the estuary through lateral input from tributaries and tidal marshes.  $\delta^{30}\text{Si}$  values in the freshwater and brackish zones were lower than in October. The most notable changes in  $\delta^{30}\text{Si}$  occurred in the tidal freshwater zone of the estuary. This underscores that this zone modulates the delivery of reactive silica from land to sea. If true for other systems estuarine transformation would significantly contribute to the long term control of the silicon isotopic composition of the ocean.

---

Responsible Editor: Leila J. Hamdan.

---

**Electronic supplementary material** The online version of this article (doi:[10.1007/s10533-015-0081-8](https://doi.org/10.1007/s10533-015-0081-8)) contains supplementary material, which is available to authorized users.

---

A. Weiss (✉) · T. Amann · J. Hartmann  
Institut für Geologie, Universität Hamburg,  
KlimaCampus, Bundesstraße 55, 20146 Hamburg,  
Germany  
e-mail: andreas.kd.weiss@gmail.com

C. De La Rocha  
CNRS UMR 6539, Institut Universitaire Européen de la  
Mer, Université de Bretagne Occidentale, Technopole  
Brest-Iroise, Place Nicholas Copernic, 29280 Plouzané,  
France

**Keywords** Silicon isotopes ·  $\delta^{30}\text{Si}$  · Dissolved silica · Elbe Estuary · Tidal marsh · Silica cycling

## Introduction

The average silicon isotopic composition ( $\delta^{30}\text{Si}$ ) of seawater largely represents the balance between inputs from continental weathering ( $\sim 68$  %), delivered mainly by rivers and high and low temperature weathering of oceanic crust ( $\sim 27$  %) (Tréguer and De La Rocha 2013). Groundwater also plays an important role of Si delivery to the oceans (Georg et al.

2009), its full extent however cannot be assessed at the moment, due to the lack of data. The oceans have an average  $\delta^{30}\text{Si}$  (around +1 ‰), which is much closer to typical riverine values (+0.5–+2 ‰) than to the values of mid-ocean ridge basalt (−0.4 ‰) or dissolved silicon (DSi) emitted by axial deep sea hydrothermal vents, suggesting the much greater input of continental Si than that from oceanic crust (Tréguer and De La Rocha 2013). However, there are severe weaknesses in both our elemental and isotopic budget for Si in the ocean, meaning that there is considerable uncertainty in these estimates. For example, we have only rough estimates for how much riverine DSi is removed in estuaries and therefore never enter the ocean (Michalopoulos and Aller 2004; Tréguer et al. 1995; Tréguer and De La Rocha 2013) and virtually no knowledge to what extent the estuarine Si cycling alters the  $\delta^{30}\text{Si}$  of reactive silica before it reaches the sea.

Estuaries serve as the interface through which solutes and reactive solids [e.g., clays and biogenic silica (BSi)] must pass during their transfer from the terrestrial biogeosphere to the ocean if delivered via rivers. These estuaries are complex environments, showing stark river to ocean gradients in turbidity, salinity, and pH (Bianchi 2007). Through colloid formation, scavenging, reverse weathering, and the production and sedimentation of biogenic materials, significant quantities of river borne solutes are retained in estuaries (Bianchi 2007), diminishing the input of these salts to seawater. Likewise, dissolution of estuarine materials (i.e., plant matter, suspended particles, or material in sediments) may at times serve as a source of solutes to the estuary, and ultimately, the ocean, for example, as shown experimentally for silica (Carbonnel et al. 2009; Pastuszak et al. 2008; Yamada and D'Elia 1984).

The Si cycling in estuaries and its effect on the elemental and isotopic Si fluxes are not well understood, and this is especially true with respect to the Si isotopes. In estuarine environments, the elemental Si flux towards the sea and its isotopic composition can be altered by various processes, such as DSi uptake and BSi production by diatoms (De La Rocha et al. 1997; Sun et al. 2013), the dissolution of BSi (phytoliths and diatom frustules) of terrestrial and aquatic origin (Demarest et al. 2009; Loucaides et al. 2008; Pastuszak et al. 2008; Yamada and D'Elia 1984), reverse weathering processes (Delstanche et al.

2009; Michalopoulos and Aller 2004; Presti and Michalopoulos 2008; Sun et al. 2014; Wetzel et al. 2014) that remove DSi during the production of clay minerals from precursors such as BSi, and the lateral input of DSi from tidal marsh areas (Struyf et al. 2006; Vieillard et al. 2011; Weiss et al. 2013).

So far there exist few  $\delta^{30}\text{Si}$  data from estuarine environments. One dataset, from the tropical Tana River Estuary, Kenya (Hughes et al. 2012), showed that the  $\delta^{30}\text{Si}$  signal was not altered along the salinity gradient of the estuary, but followed conservative mixing. Similar behavior has been observed in the San Francisco Bay Estuary at a time of the year when DSi concentrations were also conservative (De La Rocha et al. 2011). Another recent dataset covers the tributaries and the tidal freshwater part of the Scheldt River, Belgium (Delvaux et al. 2013). This study showed that the  $\delta^{30}\text{Si}$  signal in the tidal freshwater part of the estuary was altered by diatom blooms in summer. In winter the signal in the tidal river was best explained by conservative mixing with tributaries. Further variations in the  $\delta^{30}\text{Si}$  values were attributed to differences in land use and lithology on the sub basin scale.

To our knowledge, there are no other published studies of the behavior of silicon isotopes in estuaries. This general lack of data hinders the improvement of our understanding of the silica cycle in the land ocean transition zone that likely controls both the flux and isotopic composition of terrestrial Si into the ocean. To close this gap, we present here a study of  $\delta^{30}\text{Si}$  of DSi in the temperate Elbe Estuary, Germany. The data include for the first time the lateral boundary of the estuary, i.e., tidal marshes and also provides for the first time seasonal data from such areas and from the estuary itself.

## Materials and methods

### Study area

The Elbe River has the fourth largest river basin in central Europe and drains an area of approximately 148,000 km<sup>2</sup>. The mean annual long term discharge at the gauging station of Neu Darchau (536.4 km) is 704 m<sup>3</sup> s<sup>−1</sup> (average of years 1900–2011). Winter and spring discharge is higher than 700 m<sup>3</sup> s<sup>−1</sup> with the long term maximum of 1080 m<sup>3</sup> s<sup>−1</sup> in April (Kempe

1992). The Elbe's tidal Estuary is located in northern Germany and drains into the German Bight, North Sea (Fig. 1). It is a mesotidal coastal plain estuary with a maximum tidal range of 3.6 m at the Hamburg harbour. The 142 km long estuary can be divided into a freshwater, a brackish water and a saltwater stretch (Fig. 1). See Amann et al. (2012) for additional details.

Due to its importance as a seaway, the shipping channel has been deepened to the current depth of 14.9 m. The waterside has also been heavily altered by dyke construction, which led to the loss of ~55 % of dyke foreland during the last century, minimizing the area of tidal wetlands (UVU 1997, unpublished data, available at [www.portal-tideelbe.de](http://www.portal-tideelbe.de)). Roughly 79 km<sup>2</sup> of dyke foreland in the estuary remain (Fig. 1).

### Marsh sampling locations

Samples were taken at three locations along the estuarine salinity gradient (Fig. 1). The freshwater

sampling took place in the Haseldorfer Marsch (9°33.125"E, 53°39.116"N; 657 km). The tidal range at this point is 3.1 m with a mean high tide of 1.8 m above sea level (m.a.s.l. according to German height reference system, Potsdam level; BSH 2010). The marsh surface lies about 2.1 m.a.s.l. Inundation occurs only during high spring tides and storm surges. The sampling creek drains an area of 0.171 km<sup>2</sup>. Dominant vegetation (see Table 1 for details on vegetation cover) on the marsh surface are *Phalaris arundinaceae*/*Glyceria maxima* and *Phragmites australis* reeds. An artificial pond, which lies 1.6 m.a.s.l. and which is connected to the main drainage creek, is covered with *Typha* sp.

The brackish marsh site is located at the Neufelder Marsch (9°1'47.209"E 53°54'8.073"N, 703 km) at the beginning of the estuarine mouth. The tidal range at this point is 2.9 m with a mean high water of 1.5 m.a.s.l. (BSH 2010). The marsh surface has an elevation of 2.0 m.a.s.l. Only during spring tides the marsh surface can be inundated. The area is mainly

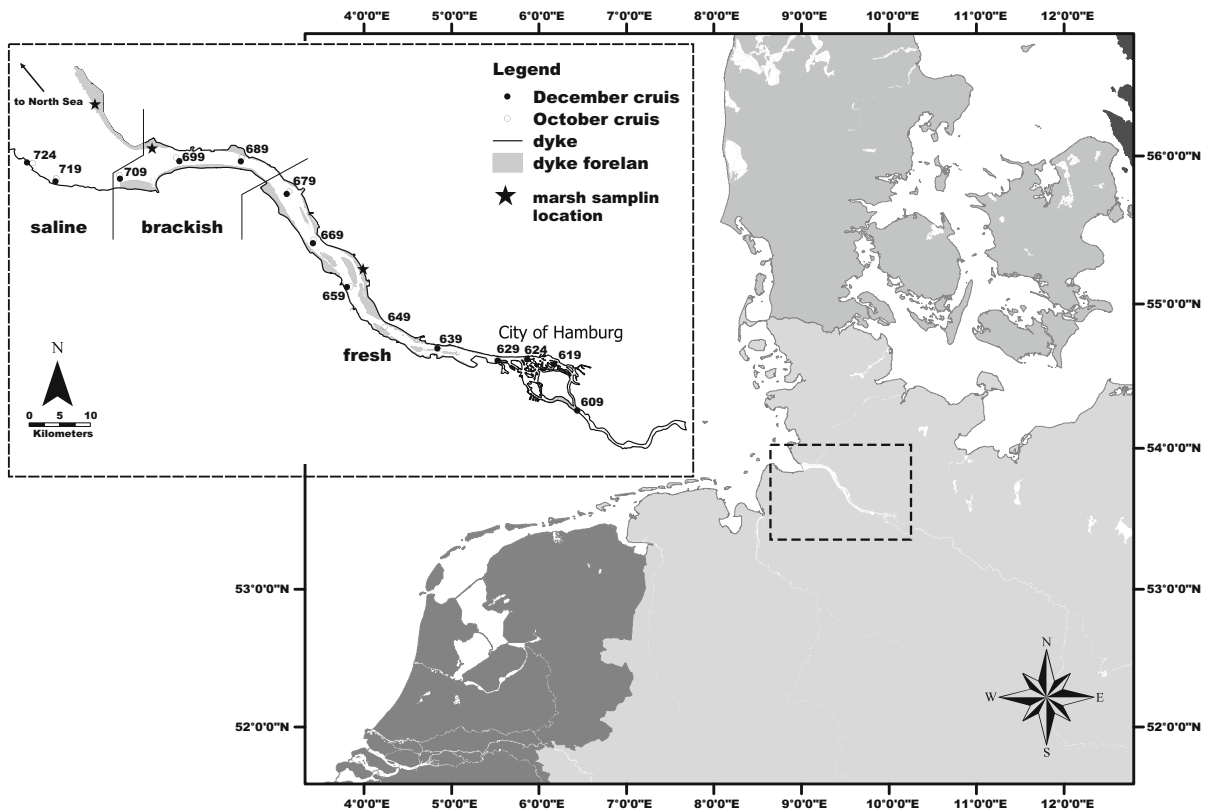


**Fig. 1** Overview of tidal marsh and estuarine sampling locations in the Elbe Estuary

**Table 1** Summary of the characteristics of the three salinity classes in which the sampling sites were located

Sampling sites	Salinity classes	Elbe (km)	Salinity <sup>a</sup>	Area (km <sup>2</sup> )	Dominant vegetation <sup>b, c</sup>	Areal proportion (%)
Fresh	Limnic	638–680	<0.5	40.58	<i>Phragmites australis</i>	37
					Trees/scrubs	30
					Mixed grassland	27
Brackish	Mixo-mesohaline	680–705	5–18	20.68	Mixed grassland	41
					<i>Phragmites australis</i>	17
					Salt meadow	15
Saline	Mixo-mesohaline/euhaline	705–721	5–30	17.90	<i>Festuca rubra</i>	22
					<i>Elymus athericus</i>	20
					<i>Puccinella maritima</i>	14
					<i>Spartina anglica</i>	13
Total				79.16		

For each salinity class possible salinity range is given as well as the dominant vegetation type of each zone. The area is the total area of the salinity class in the Elbe Estuary (see Fig. 1). Note that the species resolution of the saline sampling site is higher, because different vegetation maps were used

<sup>a</sup> Salinity characterization was taken from UVU (1997), Chap. 4, Table 4.2 (<http://www.portal-tideelbe.de/Projekte/FRA1999/Antragsunterlagen/UVU/Kartenband/index.html>)

<sup>b</sup> Data for the zones between Elbe 638 and 705 km were taken from the vegetation map “Biotopenkartierung 2006”, Zentrales Datenmanagement der WSD Nord, [www.portal-tideelbe.de](http://www.portal-tideelbe.de), May 2011. Data for the saline site were taken from the vegetation map “Salzwiesenkartierung 2006/2007”, LKN-Schleswig-Holstein/Nationalparkverwaltung

<sup>c</sup> *Italicised* species names are wetland grasses

covered by *P. australis* (45 %) and *Elymus athericus* (15 %). The sampling creek drains an area of 0.167 km<sup>2</sup>.

The salt marsh sampling took place in the Dieksanderkoog (8°52′55.674″E 53°58′26.242″N, 713.5 km) at the mouth of the estuary. The sampling site has an area of 0.568 km<sup>2</sup> and is divided by the sampling creek. The northern part of the area is grazed by sheep while the southern part was abandoned in 1990 and is no longer grazed. Vegetation on the northern side is dominated by *Festuca rubra*, the southern side by *E. athericus* meadow. The marsh surface has a mean elevation of 2.1 m.a.s.l. The tidal range in this area is 2.9 m with a mean high tide at 1.6 m.a.s.l. (BSH 2010). Even at spring tide most of the area is not inundated.

For a more detailed description of the sampling locations please refer to Weiss et al. (2013).

## Sampling

### Estuarine samples

Silicon isotope samples of the Elbe Estuary were taken with a Niskin bottle approximately 1 m below the

surface during cruises along the main axis of the Elbe Estuary on 11 October 2011 and 11 December 2011. Temperature, pH, dissolved oxygen (DO) and salinity were measured with a handheld sensor (pH, temperature: Metrohm pH 827, Primatrode 6.0228.020 or Aquatrode 6.0257.000; salinity and oxygen: WTW 350i ConOX) in a subsample. Isotope samples were filtered through 0.45 µm polycarbonate (PC) filters (Sartorius) and stored in acid cleaned opaque plastic bottles at room temperature until analysis.

### Tidal marsh samples

Samples were taken in the main creek of the sampling area on 18 May, 7 July, and 11 November 2011 at the brackish marsh, to cover seasonal variation, where the variability of DSi concentrations throughout the year was highest (Weiss et al. 2013). At the freshwater marsh and salt marsh samples were taken on 24 and 30 November 2011, respectively. For 7–12 h surface water samples were taken every hour with a plastic bottle attached to a telescoping pole to cover the seepage and the bulk phase of the tidal cycle. The seepage phase is the time during ebb tide when the water level in the creek is very low (<10 cm). The

water is a mixture of soil pore water and infiltrated estuarine water (depending on previous flooding). The bulk phase is the period of time where estuarine water is flowing in or out of the tidal creeks in great volume. In the first sample the physical parameters pH, temperature, DO and salinity were measured with a handheld sensor (same sensors named in “[Estuarine samples](#)” section). Afterwards the isotope samples were taken, filled into acid cleaned plastic bottles and stored in a cool-box. In the laboratory, each sample was vacuum filtered through a 0.45  $\mu\text{m}$  PC filter (Sartorius). The filtrate was stored in acid cleaned plastic bottles at 4 °C in the dark until analysis.

The DSi concentrations in the estuarine and tidal marsh samples were measured using standard colorimetric techniques (Strickland and Parsons 1972).

### Si isotopes

All work described here was carried out using high purity (Merck Suprapur<sup>®</sup>) acids, deionized distilled water (18.2 M $\Omega$  cm), and acid-cleaned labware (PTFE and LDPE).

DSi was precipitated from the samples applying the triethylamine molybdate (TEA-Moly) method as described in De La Rocha et al. (1996). Firstly, the DSi was precipitated overnight following the addition of the acidified TEA-Moly solution to the sample. The precipitate was collected by filtration onto a 0.6  $\mu\text{m}$  PC filter. The filter plus precipitate were then combusted in a muffle furnace using platinum crucibles. The samples were first brought to 500 °C for 2 h to remove organic compounds. The temperature was then increased to 1000 °C where it was held for 10 h to volatilize the molybdenum, leaving behind relatively pure silica (SiO<sub>2</sub>).

This silica was then dissolved in 40 % HF to yield a final Si concentration of 229.9 mM (i.e., 4  $\mu\text{mol}$  Si in 17.4  $\mu\text{L}$ ). When dissolution was complete, samples were diluted to 518.3  $\mu\text{M}$  Si and loaded onto ion exchange columns filled with AG 1-X8 resin (100–200 mesh; Eichrom) following the protocol outlined in Engström et al. (2006) and utilized previously in the lab (De La Rocha et al. 2011). A solution of 95 mM HCl plus 23 mM HF was used to elute matrix elements while Si eluted with a solution of 0.14 M HNO<sub>3</sub> plus 5.6 mM HF.

Silicon isotope abundances in the samples were measured using a Neptune multi-collector inductively

coupled plasma mass spectrometer (Thermo Scientific). Samples were diluted with 0.16 M nitric acid to 71.2  $\mu\text{M}$  Si and sample and standard beam intensities and HF concentrations ( $\sim 1$  mM HF) were matched within 10 %. The standards used were NBS28 and a laboratory working standard of 99.995 % pure silica sand (Alfa Aesar). A final concentration of 4.1  $\mu\text{M}$  magnesium was added to the samples and the standards to allow monitoring of mass fractionation during the isotopic measurements. For each measurement, beam intensities at masses 25 and 26 (Mg), and 28, 29, and 30 (Si) in dynamic mode were monitored for 1 block of 25 cycles of 8 s integrations.

Samples were first corrected for mass bias within the mass spectrometer using the deviation of the measured magnesium isotope ratio from its expected value (see Cardinal et al. 2003; De La Rocha et al. 2011 for details). Samples and standards were measured sequentially such that each sample was bracketed by a pair of measurements of a standard, with thus two samples measurements and three standard measurements making up one final number for a sample. Data are reported in delta notation relative to NBS28:

$$\delta^x\text{Si} (\text{‰}) = \frac{R_{\text{sam}} - R_{\text{std}}}{R_{\text{std}}} \times 10^3, \quad (1)$$

where  $\delta^x\text{Si}$  is  $\delta^{29}\text{Si}$  or  $\delta^{30}\text{Si}$ , and  $R_{\text{sam}}$  and  $R_{\text{std}}$  are the  $^{29}\text{Si}/^{28}\text{Si}$  (for  $\delta^{29}\text{Si}$ ) or the  $^{30}\text{Si}/^{28}\text{Si}$  (for  $\delta^{30}\text{Si}$ ) of the sample and standard.

The precision for individual measurements of  $\delta^{30}\text{Si}$  was generally  $\pm 0.04$  ‰ (1 $\sigma$  SD) on  $\delta^{30}\text{Si}$ . The long term precision (also 1 $\sigma$ ), including the column chemistry, was  $\pm 0.07$  ‰, based on 22 separate samples of the standard measured between 6 July 2009 and 1 September 2010. Both the backgrounds during analysis and the procedural blanks were normally less than 1 % of the sample signal. Final values obtained fell along the mass dependent fractionation line expected for silicon of  $\delta^{30}\text{Si} = 1.93(\delta^{29}\text{Si})$  (ESM Fig. 1).

## Results

### Tidal marsh areas

DSi concentrations in the main channels of the tidal marshes were notably higher during the seepage phase than during the bulk phase of the tide (Fig. 2). The

effect was least in the freshwater marsh, with the bulk phase concentrations averaging  $202 \pm 3 \mu\text{M}$  (i.e., the average  $\pm$  SD of all samples in the bulk phase of the tidal cycle) compared to the  $297 \pm 10 \mu\text{M}$  average of the highest concentrations during the seepage phase. In the brackish marsh, the bulk phase concentrations were generally  $<100 \mu\text{M}$  (the exact value differed with the sampling month, being lowest in May), while the maximal seepage phase concentrations ranged from roughly 300 to 460  $\mu\text{M}$ . Similarly, in the salt marsh the lowest bulk phase concentrations were  $<100 \mu\text{M}$  while the one maximal seepage phase sample had a concentration of 534  $\mu\text{M}$ . These results indicate that all of the marshes were serving as a source of DSi to the main channel.

The  $\delta^{30}\text{Si}$  values of samples from the tidal marshes fell between  $1.71 \pm 0.08$  and  $3.18 \pm 0.05 \text{‰}$  (Fig. 2) and showed different tidal signals at each sampling

location. In the freshwater marsh,  $\delta^{30}\text{Si}$  values were similar during the seepage and the bulk phase, with the five samples measured yielding an average of  $1.74 \pm 0.08 \text{‰}$  (Fig. 2). In the brackish marsh the seepage phase values were always higher than the bulk values, with the average  $\delta^{30}\text{Si}$  observed during the seepage phase being  $2.97 \pm 0.22 \text{‰}$  in May and  $2.69 \pm 0.12 \text{‰}$  in November, compared to average bulk phase values of  $2.09 \pm 0.09 \text{‰}$  in May and  $2.21 \pm 0.28 \text{‰}$  in November. These results further suggest that the values of  $\delta^{30}\text{Si}$  of DSi input from seepage are seasonally variable. In the salt marsh the pattern was reversed. Bulk phase  $\delta^{30}\text{Si}$  values ( $2.52 \pm 0.11 \text{‰}$  at the lowest DSi concentrations) were higher than the one sample from the seepage phase ( $1.81 \pm 0.03 \text{‰}$  at 534  $\mu\text{M}$  DSi).

Because both DSi concentrations and  $\delta^{30}\text{Si}$  differed between bulk and seepage phases, at most of the sites

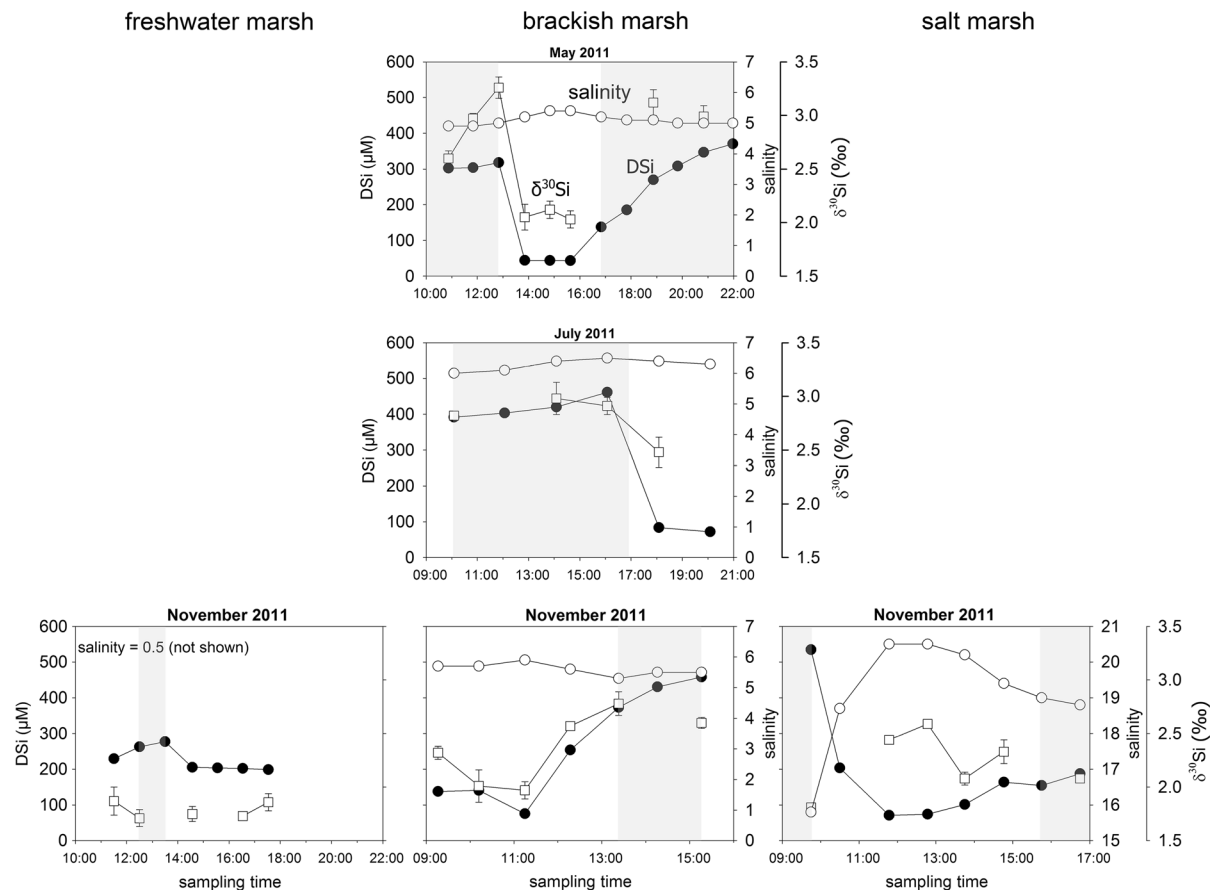


**Fig. 2** DSi concentrations,  $\delta^{30}\text{Si}$  values, and salinities at the fresh, brackish, and salt marsh sampling sites. DSi concentrations were highest during seepage phase and lowest during bulk phase. Error bars on the  $\delta^{30}\text{Si}$  data points represent  $1\sigma$  SD of duplicate analyses

distinct correlations existed between  $\delta^{30}\text{Si}$  and DSi concentrations (Fig. 3). A positive correlation was present at the brackish marsh (Pearson's  $r^2 = 0.63$ ,  $p < 0.0001$ ) while at the salt marsh the values were negatively correlated (Pearson's  $r^2 = 0.64$ ,  $p < 0.0001$ ). At the freshwater marsh no correlation was found (Pearson's  $r^2 = 0.09$ ,  $p = 0.61$ ).

## Estuarine transects

### Physical and chemical parameters

The monthly mean Elbe discharge, calculated from daily mean discharge values at the gauging station at Neu Darchau, during sampling was slightly lower in October ( $543 \pm 71 \text{ m}^3 \text{ s}^{-1}$ ) than in December ( $572 \pm 155 \text{ m}^3 \text{ s}^{-1}$ ; ESM Fig. 2). The same pattern held for the discharge on the sampling days themselves of  $419 \text{ m}^3 \text{ s}^{-1}$  (October) and  $472 \text{ m}^3 \text{ s}^{-1}$  (December). Likewise, the mean temperature of the estuary differed between October ( $10.4 \text{ }^\circ\text{C}$ ) and December ( $4.0 \text{ }^\circ\text{C}$ ).

Beyond these differences, the physical and general chemical conditions [e.g., salinity, DO saturation, pH, and concentrations of suspended particulate matter (SPM)] along the Elbe Estuary sampling transect were relatively similar between the two cruises (Fig. 4c–f). During both cruises, salinity was negligible upstream of 679 km, increasing only from 0.4 to 0.6 between 609 and 679 km. From 689 km onwards (mixing zone), the estuary became increasingly brackish due to

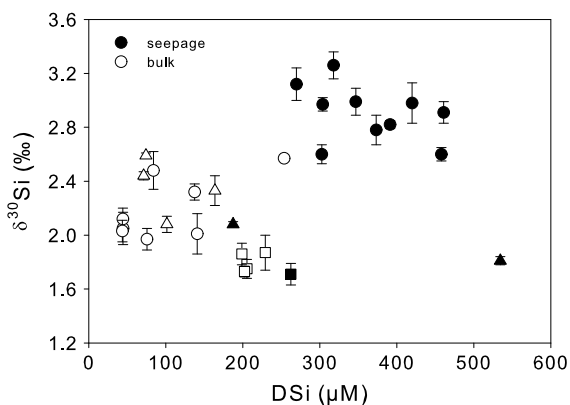


**Fig. 3**  $\delta^{30}\text{Si}$  as a function of DSi concentrations in freshwater marsh (squares), brackish marsh (circles), and salt marsh (triangles) samples. Black symbols seepage samples, white symbols bulk samples. Error bars are  $1\sigma$  SD

the increased influx of seawater, with salinities increasing to maximum of 17.7 in October and 19.4 in December towards the ocean end of the estuary (Fig. 4c). In December, the salinity decreased between 719 and 724 km due to the turning of the tidal phase from ebb tide to flood tide during the sampling. This change of the tidal flow direction was accompanied by the sampling of less saline water with higher (i.e. more river-like) DSi concentration (Fig. 4b).

### DSi concentrations and $\delta^{30}\text{Si}$

In general, during both the October and December sampling cruises, DSi concentrations decreased downstream through the estuary (Figs. 5, 6), with varying starting points of the decrease. In October, DSi concentrations decreased from  $164 \mu\text{M}$  at the furthest upstream station (609 km,  $S = 0.4$ ) down to  $52 \mu\text{M}$  at the most oceanward station (724 km,  $S = 17.8$ ; Fig. 5b). In December, DSi concentrations initially increased, rising from  $185 \mu\text{M}$  at 609 km ( $S = 0.4$ ) to a maximum of  $203 \mu\text{M}$  at 669 km ( $S = 0.6$ ). Following this, DSi concentrations decreased, reaching  $86 \mu\text{M}$  at the highest salinity (719 km,  $S = 19.4$ ).

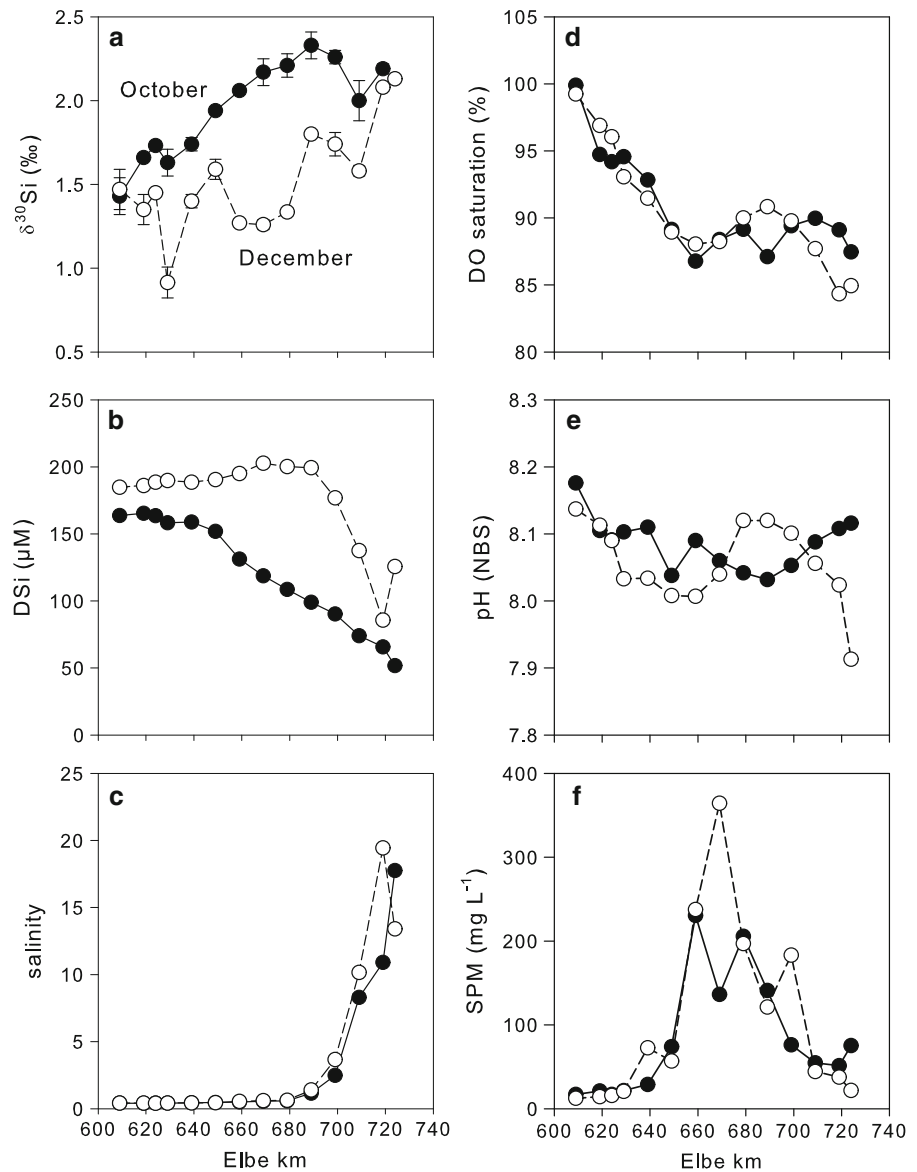
In contrast to DSi concentrations, the  $\delta^{30}\text{Si}$  of DSi generally increased downstream in the estuary along the sampling transect (Fig. 4a). The overall average  $\delta^{30}\text{Si}$  of the upstream freshwater endmember (the average of stations from 609 to 624 km) was  $1.52 \pm 0.15 \text{ ‰}$  ( $n = 6$ ), corresponding to an average of  $1.61 \pm 0.16 \text{ ‰}$  ( $n = 3$ ) in October when DSi averaged  $164 \pm 1 \mu\text{M}$  and of  $1.42 \pm 0.06 \text{ ‰}$  ( $n = 3$ ) in December when the DSi concentration at these stations averaged  $187 \pm 2 \mu\text{M}$ . In contrast, the higher salinity stations ( $S \geq 1$ ) had an average  $\delta^{30}\text{Si}$  of  $2.20 \pm 0.14 \text{ ‰}$  ( $n = 4$ ) in October and of  $1.87 \pm 0.23 \text{ ‰}$  ( $n = 5$ ) in December. At most stations, the  $\delta^{30}\text{Si}$  of DSi was lower in December than in October.

## Discussion

### Behavior of $\delta^{30}\text{Si}$ in tidal marshes

DSi present in the tidal marsh channels during the seepage phase contains DSi from the porewaters of the marsh sediments. These porewaters represent waters of different origin that have been (previously and

**Fig. 4** Physical and chemical parameters along the Elbe Estuary during the October (*filled circles*) and December (*open circles*) cruise: **a**  $\delta^{30}\text{Si}$ , **b** DSi concentration, **c** salinity, **d** dissolved oxygen saturation, **e** pH, and **f** suspended matter concentration. *Error bars* for the  $\delta^{30}\text{Si}$  values are  $1\sigma$  SD. Elbe km denotes the distance from the Czech border



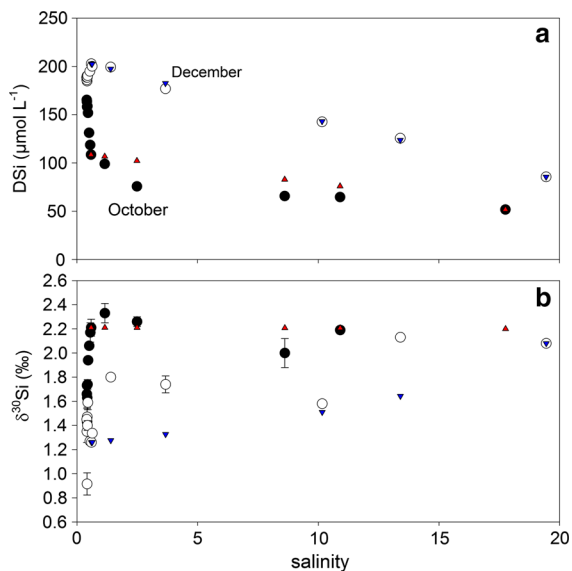
afterwards) subject to any of a numerous set of biogeochemical processes. Isotope fractionation upstream, downstream, and within the marshes combined with mixing control the  $\delta^{30}\text{Si}$  of the porewaters at any given time.

Figure 7 provides visual guidance for the discussion of the isotopic silica cycling in the tidal marsh areas in “[The potential influence of hydrology](#)” and “[The potential influence of silica cycling within the marshes and marsh soils](#)” sections and offers a rough overview of the factors influencing the isotopic Si cycle in tidal marshes.

#### *The potential influence of hydrology*

The Elbe Estuary has a semidiurnal flooding regime with two tides approximately every 25 h (BSH 2010). Most high tides flood only the tidal creeks and do not inundate the marsh surface. No infiltration of this water occurs into the marsh soil because the hydraulic pressure gradient between the soil and the creek allows infiltration only if the inundation water level exceeds the marsh surface (Gardner 2005a). However, inundation of the marsh soil to this critical depths can occur between September and March when storm surges





**Fig. 5** **a** DSi and **b**  $\delta^{30}\text{Si}$  as a function of salinity during the October (filled circles) and December (open circles) cruise. Inverse red and blue triangles represent DSi and  $\delta^{30}\text{Si}$  values from conservative mixing from the October and December cruise, respectively. Error bars are  $1\sigma$  SD. (Color figure online)

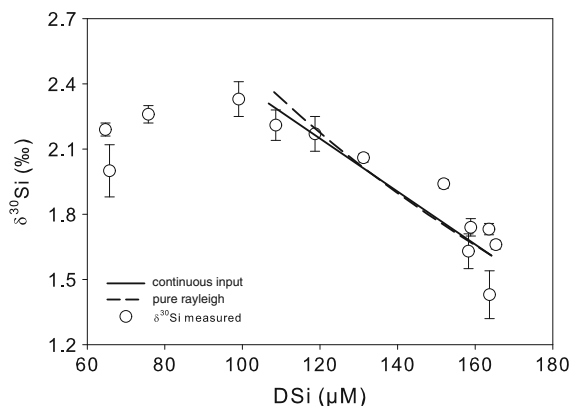


**Fig. 6** Isotope fractionation during DSi removal along the October cruise transect. Squares represent the measured  $\delta^{30}\text{Si}$  signal of DSi between 609 and 679 km, the error bars represent  $1\sigma$  SD. The lines show the theoretical evolution of  $\delta^{30}\text{Si}$  under continuous input and Rayleigh distillation models. The average DSi concentration and  $\delta^{30}\text{Si}$  value of 609–624 km ( $n = 3$ ) was used for the starting conditions

flood the marsh. All other things being equal, such infiltration should decrease the porewater concentration of DSi and shift its  $\delta^{30}\text{Si}$  towards a “marine” direction and generally pump DSi out of the tidal marsh with increased seepage discharges.

Ordinarily, the seepage water in the tidal marshes, which drains into the tidal creek, is drawn from the

pool of soil porewater within several meters of the edge of the tidal creek (Gardner 2005a). Because of the constant drainage, this water has shorter turnover times than the soil porewater in the center of the marsh and thus, one might predict a lower DSi concentration and a less extreme isotopic composition.

The hydrological conditions of the sampling site at the time of sampling is the likely reason that, unlike in the brackish and salt marshes, the  $\delta^{30}\text{Si}$  of the seepage sample ( $1.71 \pm 0.08$  ‰) in the freshwater marsh did not differ from those of samples taken during the bulk phase (average =  $1.80 \pm 0.07$  ‰;  $n = 4$ ). The seepage sample consisted mainly of bulk phase water that had infiltrated into the marsh soil during flooding in the days and hours prior to sampling. In this case, hydrology would be considered the dominant factor affecting  $\delta^{30}\text{Si}$  of seepage at the freshwater site.

The freshwater marsh soil has higher saturated water conductivity than the soils of the other two marshes (UVU 1997, unpublished data, available at [www.portal-tideelbe.de](http://www.portal-tideelbe.de)) and was flooded on three consecutive days (26th–28th November) prior to the sampling day (30th November) and in the hours immediately preceding sampling. The inundation depth of the marsh surface was 0.50–1.7 m. Under these conditions, infiltration of the overlying water into the marsh soil is known to occur (Fischer 1994; Gardner 2005a, b), replacing porewaters with water from the overlying flood. As a result of this infiltration of water into the soil, the water discharge out of the marsh during the seepage phase was much higher than on days without prior flooding (ESM Fig. 3). This sponge effect of marsh soil soaking up infiltration water and then releasing the excess during seepage has also been reported by another study of tidal marshes in the German Wadden Sea National Park (Müller et al. 2013). However, we would not expect hydrology to be controlling the  $\delta^{30}\text{Si}$  of seepage out of the brackish marsh or the salt marsh as they did not experience inundation during the 68–70 days prior to sampling. It is unsurprising, then, that the  $\delta^{30}\text{Si}$  of the seepage phase in these two marshes is both higher than in the freshwater marsh and quite different from the values during the bulk phase of the tide.

#### *The potential influence of silica cycling within the marshes and marsh soils*

Assuming that the  $\delta^{30}\text{Si}$  of DSi in the tidal creeks at the end of the seepage phase approaches the  $\delta^{30}\text{Si}$  of the

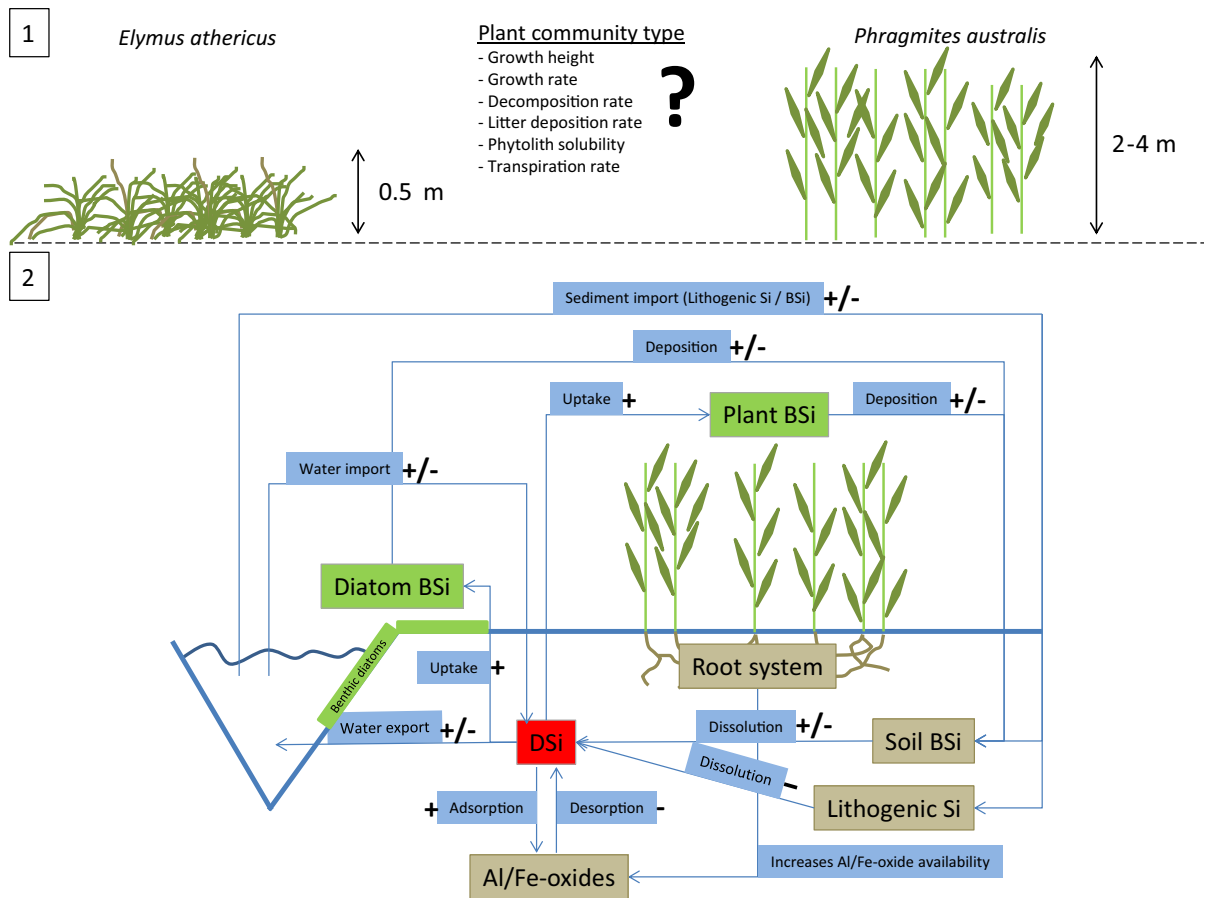


**Fig. 7** Schematic of factors and processes influencing the isotopic Si cycle in the tidal marsh areas of the Elbe Estuary. The upper panel 1 visualizes the morphological differences of an *Elymus athericus* salt marsh and the *Phragmites australis* freshwater and brackish marsh. The double headed arrows indicate typical growth heights of the species. Listed are factors that may influence the isotopic Si cycling in the marsh. The lower panel 2 shows the processes and factors that were discussed throughout “The potential influence of hydrology”–

“Isotope fractionation associated with net removal of DSi in October” sections and their influence on the isotopic signature of the soil porewater DSi (red box). The “+” indicates an enrichment of  $^{30}\text{Si}$  in the porewater, the “–” a depletion of  $^{30}\text{Si}$ . The “+/-” indicates that the direction of change in the  $\delta^{30}\text{Si}$  value of the soil porewater DSi can either have an decreasing or increasing effect on the  $\delta^{30}\text{Si}$  value, depending on factors like the  $\delta^{30}\text{Si}$  value of imported sediments or phytoliths of plant matter. (Color figure online)

tidal marsh porewaters, the generally elevated  $\delta^{30}\text{Si}$  of the creeks of the brackish marsh during the seepage phase suggest that the porewaters contain DSi with  $\delta^{30}\text{Si}$  of at least 2.6 ‰ to more than 3 ‰ (Fig. 2). The  $\delta^{30}\text{Si}$  values of up to 3.2 ‰ measured during the seepage phase of the brackish marsh, if accepted as reflecting the marsh soil solution, would be the highest reported so far for soil solutions, which generally range from  $-1.1$  to  $2.1$  ‰ (Opfergelt and Delmelle 2012). To put these values  $\geq 3$  ‰ into an even broader perspective, they sit at the upper end of those reported for rivers, lakes, groundwater, and the ocean, which generally range from 0.5 to  $\sim 3.5$  ‰ (Alleman et al.

2005; Cardinal et al. 2010; De La Rocha et al. 2000; Ding et al. 2004, 2011; Ehlert et al. 2012; Fontorbe et al. 2013; Georg et al. 2006, 2009; Hughes et al. 2012; Opfergelt et al. 2011; Reynolds et al. 2006; Sun et al. 2013; Varela et al. 2004).

Mineral weathering and other biogeochemical cycling of silicon in soils strongly affects the  $\delta^{30}\text{Si}$  of DSi in the soil porewaters (soil solutions). This can be due to the dissolution of solid phases which may have very particular isotopic compositions. In addition, fractionation of silicon isotopes may occur during many reactions, such as the dissolution of primary silicate minerals, the precipitation or dissolution of secondary

minerals, and net removal of silicic acid ( $\text{Si}(\text{OH})_4$ ) to solid phases or exchange between silicic acid and minerals such as clays, oxy-hydroxides, and amorphous (usually biogenic) silica (Basile-Doelsch 2006; Michalopoulos and Aller 2004; Opfergelt and Delmelle 2012; Ziegler et al. 2005). Additionally, fractionation of silicon isotopes during the uptake of DSi to form BSi by plants that produce silica phytoliths (Opfergelt et al. 2006), and by silicifying microorganisms (including but not limited to diatoms) could also affect the  $\delta^{30}\text{Si}$  of the porewaters and the seepage water in the tidal creeks (e.g. De La Rocha et al. 1997; Ding et al. 2005). The fractionation effects associated with BSi dissolution are still not fully understood. Demarest et al. (2009) found discrimination against heavy isotopes, while Wetzel et al. (2014) found no dissolution effect at all. Sun et al. (2014) found a fractionation effect at the early stage of dissolution only in the DSi, which  $\delta^{30}\text{Si}$  signal decreased by  $-0.86\text{‰}$ . Roughly speaking, precipitation of secondary minerals and biogenic phases increases the  $\delta^{30}\text{Si}$  of the DSi while dissolution of them decreases it for the reasons outlined above. The initial effects of these processes on the  $\delta^{30}\text{Si}$  of the fluids can be augmented by successive dissolution/precipitation or adsorption/desorption cycles (Opfergelt and Delmelle 2012). Finally, soil hydrology also plays its part, due to its influence on the mixing of different water masses with potentially quite distinct  $\delta^{30}\text{Si}$  values.

Given the  $\delta^{30}\text{Si}$  values during seepage in the brackish marsh elevated are above the  $\delta^{30}\text{Si}$  values found in the estuary (1.3–2.2 ‰, excluding the two most extreme data points), silica cycling in this tidal marsh or within the soils themselves has had the general effect of increasing the  $\delta^{30}\text{Si}$  in the porewaters. This could reflect a greater extent of removal of DSi to abiotic and/or biogenic solid phases (a possibility, which is not excluded by the concentrations of DSi in the seepage waters of more than 300  $\mu\text{M}$ ). Alternatively, it might indicate adsorption reactions, which favor the retention of the lighter isotope over the heavier one on the surface of the solid phase. Or it may suggest that dissolving solids (clays, BSi) have a relatively high  $\delta^{30}\text{Si}$ . We consider these possibilities below.

*The potential influence of marsh vegetation* Silicon cycling in tidal marshes is strongly influenced by vegetation (Struyf and Conley 2009, 2011; Struyf et al.

2005, 2006, 2007). It is likely that the cycling of silicon isotopes through tidal marshes is also heavily affected by vegetation.

Monocots (such as grasses) favour the incorporation of lighter silicon isotopes over the heavier ones during the uptake of DSi and production of silica phytoliths, as shown for banana (Opfergelt et al. 2006), bamboo (Ding et al. 2008b), rice (Ding et al. 2005, 2008a), wheat, and corn (Ziegler et al. 2005). Fractionation of Si isotopes for the overall process of DSi uptake, transport within the plant, and phytolith precipitation appears similar for these species, with a value of about  $-1\text{‰}$  (n.b.: similar also to what is known for silica biomineralization by diatoms).

Tidal marshes are grassland ecosystems dominated by species such as *P. australis*, *E. athericus*, *Typha* spp., *Spartina* spp. and *P. arudinaceae*, which all are species known for their accumulation of silica (Raven 2003). In these plants, a portion of the DSi taken up through the roots is precipitated in a controlled fashion as BSi in specific, taxonomically-distinct bodies known as phytoliths (Kaufman et al. 1981). Silicon isotopes are fractionated during this process, resulting in silica phytoliths with a  $\delta^{30}\text{Si}$  that is lower than the DSi available to the plants (Ding et al. 2005, 2008a, b; Opfergelt et al. 2006). The BSi content of tidal wetland plants can reach values of about 70  $\text{mg g}^{-1}$  dry weight, which is comparable to that of rice (Struyf and Conley 2009, electronic supplemental material), and thus represents a considerable (and dynamic) reservoir of silicon in tidal marsh systems (Struyf et al. 2005).

The common reed, *P. australis*, a significant species in tidal marshes, in particular contains up to 10 wt-% BSi (Struyf et al. 2009, electronic supplement material). The storage of BSi in *P. australis* in a tidal freshwater marsh in the Scheldt Estuary, Belgium, alone accounted for 90 % of all BSi found in vegetation in the marsh (Struyf and Conley 2009). This BSi is several orders of magnitude more soluble than clay minerals, primary mafic silicates, and feldspars (Frayse et al. 2009) and as a result it has short turnover times compared to other particulate silica components of soils. For example, it has been shown for a tidal freshwater marsh that 50 % of the BSi in litter of *P. australis* was dissolved after only 20 days and 98 % dissolved within the space of a year under typical conditions for the marsh (Struyf et al. 2007). In this particular marsh the reed decomposition was accountable for 40 % of the marsh DSi export.

Through their removal of DSi from marsh soils and their production of phytoliths with a relatively low  $\delta^{30}\text{Si}$ , *P. australis* and other marsh plants have the potential to create high  $\delta^{30}\text{Si}$  values in the tidal marsh soil solutions. The uptake of DSi and production of phytoliths and their associated isotope fractionation would increase the  $\delta^{30}\text{Si}$  of the DSi remaining behind in the soil solution. This would be especially true during times of the year when the plants are most actively growing, increasing the size of the low  $\delta^{30}\text{Si}$  phytolith reservoir within a marsh. During times of the year when dissolution of these phytoliths (e.g., from plant litter) is greater than their production, however, recycling of the phytolith silicon would likely lower the  $\delta^{30}\text{Si}$  of DSi, if not in the soil solutions, than in the overlying waters of the marshes.

However, isotopically speaking, the recycling of phytoliths is a complex issue. Due to the successive increase of  $\delta^{30}\text{Si}$  of the unreacted pool of DSi as it moves upwards from the roots, the  $\delta^{30}\text{Si}$  of phytoliths in lower parts of the plant (for *P. australis*, this would be in the stem) should be lower than in the ones produced in the leaves and seeds (as shown for rice in the laboratory and observed in the field in bamboo and rice by Ding et al. (2008a)). As phytoliths in the stems are retained within the plant for significantly longer than those in leaves or seeds, recycling of Si from phytoliths should predominantly favor the dissolution of phytoliths of higher  $\delta^{30}\text{Si}$ , allowing the plants to serve as a slightly longer lived sink of low  $\delta^{30}\text{Si}$  phytoliths. This could contribute to the  $\delta^{30}\text{Si}$  enrichment of the soil porewaters and help to explain the high values observed in the brackish marsh.

The lower  $\delta^{30}\text{Si}$  values during the seepage phase at the salt marsh compared to the brackish marsh in November could indicate a weaker influence of the vegetation on the isotopic composition in the seepage water. While in the brackish marsh a tall growing species (*P. australis*) dominates, which is known for its high transpiration rates and high BSi contents, the salt marsh is dominated by *E. athericus*. This grass does not grow stems as high as *P. australis* does, but forms a dense leaf cover of 0.3–0.5 m in height, with high potential for self-shading. Lower BSi contents compared to *P. australis* (Weiss et al. 2012, Table 4), may indicate differences in Si uptake rates, possibly due to the self-shading effect (see Fig. 7 for a comparison of these two plant communities). Additionally, the growth form of *E. athericus* would

decrease the phytolith retention time in the plant after the vegetation period. Due to the lack of understanding of the inputs and outputs of BSi and DSi and their respective  $\delta^{30}\text{Si}$  values, as well as a lack of knowledge of the hydrology of the main creeks catchment, this explanation is very speculative. Future studies are needed to improve our process understanding of different plant communities on the isotopic Si cycle.

*The potential effects of adsorption and desorption of DSi onto oxides* Adsorption of DSi onto iron (Fe; Delstanche et al. 2009) and aluminum (Al; Oelze et al. 2014) oxides is accompanied by isotopic fractionation and could be an important part of the silica cycling in marshes. Lighter isotopes are preferentially adsorbed, driving an increase in the  $\delta^{30}\text{Si}$  of DSi. For Fe oxides the adsorption is pH dependant and reaches its maximum around pH 9 (e.g., Hiemstra et al. 2007; Jones and Handreck 1963). Al oxides are twice as effective as iron oxides at adsorbing Si (Jones and Handreck 1963).

The redox state of tidal marsh soils and therefore the availability of Fe oxides are governed by hydrological and biogeochemical factors, which interact in a complex way. For example, on the one hand, inundation reduces the oxygen availability due to the low oxygen diffusion in water compared to a porous medium like a well-drained soil (c.f. Mitsch and Gosselink 1993, p. 120), resulting in reducing conditions favoring the formation of iron sulphides. On the other hand, infrequent flooding paired with low precipitation and high temperatures cause the drying of the marsh soil and can even cause desiccation cracks, allowing atmospheric oxygen to penetrate into the soil. As a result, the oxidation of Fe sulphides to Fe oxides is favored. Furthermore, the formation of Fe oxides is regulated by plants, via the effect of root aeration on the availability of poorly crystalline Fe for microbial Fe reduction (Weiss et al. 2004). As the fractionation factor related to absorption on Fe oxides is positively related to their crystallinity (Delstanche et al. 2009), the presence of plants may decrease the influence of adsorption on the  $\delta^{30}\text{Si}$  of DSi in the soil porewater.

It can be assumed that the factors, which increase the availability of Fe oxides in the marsh soil are more prevalent in warmer months (i.e., May and July, but not November), because at those times conditions favor processes responsible for oxygenation of the soil

(dense vegetation cover, better soil drainage, desiccation cracks) and thus oxidation of Fe. Hence, the influence of adsorption on  $\delta^{30}\text{Si}$  values of the marsh porewater in the November samples from all marshes was most likely small. However, detailed studies are needed to quantify the effect of the adsorption/desorption process on the  $\delta^{30}\text{Si}$  of DSi in pore and seepage waters in tidal marshes.

### Elbe Estuary

These  $\delta^{30}\text{Si}$  values represent the first values measured for the Elbe Estuary and only the third dataset from estuarine systems (Delvaux et al. 2013; Hughes et al. 2012). As such, they provide some of our first insights into the influence of the estuarine transition on the  $\delta^{30}\text{Si}$  of DSi delivered from the continents (via rivers) to the sea. The  $\delta^{30}\text{Si}$  data from both the October and December estuary transects, during which the  $\delta^{30}\text{Si}$  of DSi increased downstream by 0.4–0.6 ‰ show that the  $\delta^{30}\text{Si}$  that enters the estuary can be altered by processes occurring in the estuary. This is something, which must be taken into account in silicon isotopic budgets for the ocean and how the average  $\delta^{30}\text{Si}$  of seawater might change over time. For example, Georg et al. (2006) showed that a small offset of +0.2 ‰ from the average riverine  $\delta^{30}\text{Si}$  of 1.0 ‰ would change the average continental input significantly from 0.8 to 0.98 ‰ and therefore change the Si isotopic input into the oceans (De La Rocha and Bickle 2005; Georg et al. 2006). This is especially important for estuaries because they are features of transgressive sealevels (and are thus not a continuously present feature of continental shorelines; Dalrymple and Choi 2007). Due to transgression in the 20 kyr since the Last Glacial Maximum, for example, the present day is marked by a considerably above average number of estuaries compared to much of the geologic past (Kennett 1982). Globally, the Elbe Estuary might not be of significance for the Si cycle, because important rivers and their estuaries (in terms of Si delivery to the ocean) are located in the tropics and subtropics (Beusen et al. 2009; Dürr et al. 2011; Hartmann et al. 2010). Therefore future studies should focus on these locations. However, it is a good representation for temperate European estuaries, due to similar biogeochemical properties, which are shared with the Thames Estuary (Tinsley 1998), Delaware Estuary (Sharp 2010; Sharp et al. 1982), and the Scheldt Estuary (Soetaert et al. 2006) and as such a

good starting point to study the isotopic silica dynamics in estuaries.

### *Isotope fractionation associated with net removal of DSi in October*

A shift in the isotopic composition of a reservoir (e.g., DSi in the estuary) induced by a removal process (e.g., BSi production) that fractionates isotope ratios is often described using either of two simple models: The Rayleigh model for distillation of isotope ratios within a system where the DSi output (i.e., BSi production) is much lower than the DSi input, and the continuous input model where input and removal processes are of similar magnitude (also called the closed and the open system model, respectively):

$$\text{Rayleigh: } \delta^{30}\text{Si} = \delta^{30}\text{Si}_0 + \varepsilon(\ln(f)), \quad (2)$$

$$\text{Continuous input: } \delta^{30}\text{Si} = \delta^{30}\text{Si}_0 - \varepsilon(1 - f), \quad (3)$$

where  $f$  is the fraction of DSi remaining at the cessation of uptake, and  $\delta^{30}\text{Si}_0$  is the silicon isotopic composition of the initial DSi source. The  $\delta^{30}\text{Si}_0$  used in this study represented the average of the highest upstream sampling stations 609, 619, and 624 km of the October cruise. Finally,  $\varepsilon$  is the Si fractionation factor for diatoms relative to DSi expressed in permil.

Using the continuous input model, which would represent a situation where DSi was put into the estuary continuously along the flow path from the sides or sediments, as well as coming from upstream, the  $\varepsilon$  estimated was  $-2.0$  ‰ (Fig. 6). For the Rayleigh distillation model, which would represent a system, where the only source of DSi was from upstream, the estimated  $\varepsilon$  was  $-1.8$  ‰.

These values compare well to other estimates of silicon isotope fractionation by diatoms. For example, several authors have examined fractionation by individual marine diatom species in laboratory experiments, yielding results that ranged from  $-0.54$  to  $-2.1$  ‰ (De La Rocha et al. 1997; Milligan et al. 2004; Sutton et al. 2013). In productive marine environments fractionation of silicon isotopes during diatom growth has been estimated from depth profiles of DSi and  $\delta^{30}\text{Si}$  to be roughly  $-1.1$  ‰ (De La Rocha and Bickle 2005; Fripiat et al. 2011). Isotope fractionation associated with DSi removal by natural freshwater diatom assemblages has also been estimated at  $-1.1$  to  $-1.6$  ‰ (Alleman et al. 2005; Sun et al. 2013).

The distribution of DSi along the estuary measured during the October transect (Fig. 4b) is comparable to those from monitoring data measured in October in 1992–2009 (FGG Elbe 2012). For example, the main feature of the DSi concentrations along the October transect is their sharp decline beginning around 640 km (Fig. 4b). Ten out of the 15 years of monitoring datasets also show a distinct decrease of DSi concentrations after 640 km. This autumn drawdown of DSi concentrations is thus a common occurrence in the Elbe Estuary. Simple dilution can be ruled out as a cause due to concentrations of DSi in the tributaries feeding into the main channel of the estuary being higher year round than in the main channel itself (Amann et al. 2014). Diatom production and adsorption are two processes that could be responsible for the observed DSi concentration decrease.

The net DSi loss in the freshwater zone (calculated from the difference between the DSi concentrations at 639 and 679 km and the water volume of this zone) totals 28.55 kmol DSi. Although DSi uptake and BSi production by diatoms in the Elbe Estuary was not measured, it is possible to roughly estimate the rates of DSi uptake by extrapolating from rates of primary production (numbers were rounded the first decimal). Rates of primary production by pelagic phytoplankton in the maximum turbidity zone of Elbe Estuary measured in April were reported as 1.7–4.2 mmol C m<sup>-2</sup> day<sup>-1</sup> (Goosen et al. 1999). Diatoms represent 50–95 % of the phytoplankton population in the Elbe Estuary (Wolfstein and Kies 1995). Taking 50 % as a conservative estimate for this calculation the diatomaceous rate of primary production would be 0.85–2.1 mmol C m<sup>-2</sup> day<sup>-1</sup>. Assuming further, that the primary production rates are higher in April than in October due to the physiological state of the phytoplankton community, this estimate is most likely an overestimation of the diatomaceous primary production in October. Primary production rates can be converted into DSi uptake rates by assuming a molar Si:C ratio of 0.4. This value represents the minimum value (average-SD = 0.79–0.43, rounded to 0.4; Sicko-Goad et al. 1984 as cited in Conley et al. 1989) of 12 freshwater diatom species. The resulting rates of DSi uptake could be then multiplied with the surface area of the DSi loss zone (63.42 km<sup>2</sup> between 639 and 679 km, only deep water and the shipping channel considered) to yield a total DSi uptake in this

zone of 2.0–5.1 kmol Si day<sup>-1</sup>. Under these conditions, the total DSi loss of 28.55 kmol DSi between 639 and 679 km would be achievable in 5–14 days. This is a reasonable number considering a mean water residence time of about 16 days between 639 and 680 km under the prevailing discharge conditions (Bergemann et al. 1996). Additionally, DSi uptake could have taken place in the shallower, less turbid side branches of the estuary, where light is less limiting to phytoplankton growth than in the main stream (Kerner 2007). However, supplemental data of NO<sub>3</sub><sup>-</sup> and PO<sub>4</sub><sup>3-</sup> concentrations (ESM Fig. 4), taken at the same cruise, showed, that the DSi decrease was not accompanied by a stoichiometric decrease of these nutrients, as would be expected during phytoplankton production. Nitrate concentrations decreased by 13 μM (from an initial concentration of 132 μM) between 660 and 680 km, which is 20 km downstream of the onset of the DSi decrease. PO<sub>4</sub><sup>3-</sup> concentrations did not change in the zone of DSi decrease. It is therefore not obvious that diatomaceous BSi production have caused the decrease of DSi concentrations.

One alternative is that the DSi concentrations decreased along the transect due to adsorption of Si onto SPM in the estuary. In October (as in December) SPM concentrations began to increase notably from 639 km and showed maximal values generally between 659 and 679 km before tailing off over the rest of the transect (Fig. 4f). The mineral phase of suspended matter in the Elbe Estuary consists of mainly silt <20 μm (70 wt%) and clay <2 μm (30 wt%) (Schwedhelm et al. 1988). At a weight fraction of 50 %, illite is the dominant mineral in the 2–20 μm fraction followed by kaolinite and chlorite at ~20 % each. The clay fraction <2 μm also consists of illite (~45 wt%), kaolinite (~20 wt%) and chlorite (~10 wt%), but also contains ~20 wt% smectite (Schwedhelm et al. 1988), the formation of which from such precursor clay minerals would have removed some DSi from solution. The SPM composition has thus the prerequisites for DSi adsorption onto aluminum oxide surfaces of the clay minerals.

Assuming the removal of DSi is solely due to the adsorption of DSi onto clay mineral surfaces, the adsorption capacity of the SPM must be as high as 309 mmol kg<sup>-1</sup> to account for the loss of 28.55 kmol Si, assuming an average SPM concentration of 161.6 mg L<sup>-1</sup> between 639 and 679 km. This value

exceeds all adsorption capacity measurements that have made for metal ions (e.g., Manning and Goldberg 1996) or DSi (Delstanche et al. 2009) on clay minerals by at least three orders of magnitude. To come close to the adsorption capacity cited in the literature, the SPM concentration in this zone would have to have been  $>1000 \text{ mg L}^{-1}$ . These values do occur in nature in fluid mud systems like in the Gironde Estuary (Abril et al. 2000). SPM concentrations in the Elbe Estuary rarely exceed  $300 \text{ mg L}^{-1}$  (FGG Elbe 2012) in the surface water but can be up to six times higher near the sediment (Goosen et al. 1999). Adsorption on sediment particles is thus most likely not the main cause for the decline of DSi concentrations and the increase of  $\delta^{30}\text{Si}$  values in the freshwater part of the estuary, but may be—in concert with diatom uptake—responsible for the observed variations. It is also worth noting that similarly high (if not higher) SPM concentrations during the December transect did not result in a clear, sustained increase in  $\delta^{30}\text{Si}$  in this zone (Fig. 4f).

In conclusion we can say that our data does not allow for an identification of the main cause for DSi decrease. It is most likely that neither diatom BSi production nor adsorption are the sole processes that induce the changes of  $\delta^{30}\text{Si}$  in the complex biogeochemical setup of the estuary but an interplay of multiple factors cause the observed pattern.

Whatever process removed DSi in this stretch of the Elbe Estuary, the overall isotope fractionation associated with it, as calculated from these two simple models, was  $-1.8$  to  $-2.0$  ‰.

As shown by this dataset the interplay of multiple processes involved in the estuarine Si cycle and the complex spatio-temporal patterns of estuarine biogeochemical cycling prevents an straight forward identification and description of the cause of DSi concentration changes. Better experimental setups and sampling strategies of future studies are needed to describe the estuarine isotopic silica cycle in the Elbe Estuary and other estuaries around the world. This is an important task because up to date riverine  $\delta^{30}\text{Si}$  values are used in modeling studies concerning the oceanic isotopic Si cycle. Special focus should be laid on tropical estuaries and volcanic islands as these are the hot spots for DSi delivery to the ocean (Beusen et al. 2009; Dürr et al. 2011; Hartmann et al. 2010).

### *The lack of comparable DSi decrease and $\delta^{30}\text{Si}$ increase in December*

The distribution of DSi in the Elbe Estuary during December, with concentrations increasing until roughly 669 km (when increasing salinities indicated dilution with seawater) was typical for this time of year as shown by monitoring data from 1992 to 2009 (FGG Elbe 2012). Increasing water residence time with distance downstream paired with lateral DSi input from tidal marshes (Weiss et al. 2013) and tributaries (Amann et al. 2014) (ESM Fig. 4) could have led to the observed increase in DSi along the estuary up to this point. Additionally, high rates of organic matter remineralisation in the maximum turbidity zone could have enhanced rates of BSi dissolution in this zone (by stripping the silica of its protective organic matter cover; Bidle 1999; Bidle and Azam 2001) and thus also contributed to the increase in DSi concentration. However, the low water temperatures in December ( $4$  °C) would have minimized rates of silica dissolution as they are highly temperature dependent (Kamatani 1982), making the contribution of BSi dissolution to the increasing DSi concentrations in this zone most likely minimal.

In terms of  $\delta^{30}\text{Si}$  over the entire freshwater region (609–679 km) of the estuary in December, the values, while slightly noisy, do not show systematic variation. Excluding the anomalously low value of 0.92 ‰,  $\delta^{30}\text{Si}$  over this part of the transect averages  $1.39 \pm 0.11$  ‰ ( $n = 6$ ). This closely matches the value measured for the most upstream station (609 km) in October ( $1.43 \pm 0.11$  ‰), the station prior to the drop in DSi concentration and increase in  $\delta^{30}\text{Si}$  associated with the autumn growth of diatoms in the estuary (see “[Isotope fractionation associated with net removal of DSi in October](#)” section). As such, it may represent the general “riverine” value of  $\delta^{30}\text{Si}$  input into the Elbe Estuary.

As DSi is mixed conservatively with water from the German Bight the high  $\delta^{30}\text{Si}$  values measured at 720 km suggest that the  $\delta^{30}\text{Si}$  values in the German Bight are higher than the average seawater. This may be caused by the water exchange of the Wadden Sea and the sediment itself, as the German Bight is not very deep. It is known that DSi is exported from the

Wadden Sea back barrier areas (Grunwald et al. 2010) is derived from porewater of the tidal flats. There, the  $\delta^{30}\text{Si}$  values of this water could have been increased by adsorption processes and clay formation, resulting in higher  $\delta^{30}\text{Si}$  values than normally observed in offshore seawater. This, however, remains speculative because  $\delta^{30}\text{Si}$  data from the Wadden Sea area are currently missing.

## Conclusions

Silica cycling in the Elbe Estuary alters the silicon isotopic composition of DSi being transported through it to the ocean, especially during times of the year of most likely biological net DSi removal. This finding is new and of key importance to the long term control of the silicon isotopic composition of the ocean. It underlines the importance of estuaries in modulating the delivery of reactive silica from the continents to the ocean. The most notable changes in  $\delta^{30}\text{Si}$  occurred in the tidal freshwater zone of the Elbe Estuary, which highlights the significance of this zone for biogeochemical transformations of silica in tidal estuaries. On a global scale estuaries could thus be able to significantly change the riverine Si isotopic input into the oceans and exert a major influence on the whole oceanic  $\delta^{30}\text{Si}$  signal.

**Acknowledgments** We would like to thank Tom Jäppinen for great assistance during the field campaigns. We are grateful to captain and crew of the R/V Prandtl for their professional work and to Volker Dzaak for organising the necessary ship time. Three anonymous reviewers helped to improve the manuscript. Andreas Weiss was funded by ESTRADE (Estuary and Wetland Research Graduate School Hamburg as member of LEXI (State Excellence Initiative) and by the DFG Cluster of Excellence ‘CliSAP’ (EXC177). Thorben Amann and Jens Hartmann were funded by the DFG Cluster of Excellence ‘CliSAP’ (EXC177).

## References

Abril G, Riou SA, Etcheber H, Frankignoulle M, de Wit R, Middelburg JJ (2000) Transient, tidal time-scale, nitrogen transformations in an estuarine turbidity maximum—fluid mud system (The Gironde, South-west France). *Estuar Coast Shelf Sci* 50(5):703–715

Alleman LY, Cardinal D, Cocquyt C, Plisnier PD, Descy JP, Kimirei I, Sinyinza D, Andre L (2005) Silicon isotopic fractionation in Lake Tanganyika and its main tributaries. *J Gt Lakes Res* 31(4):509–519

Amann T (2013) Spatio-temporal variability of carbon and silica fluxes through the Inner Elbe Estuary. Staats- und Universitätsbibliothek Hamburg, Hamburg

Amann T, Weiss A, Hartmann J (2012) Carbon dynamics in the freshwater part of the Elbe Estuary, Germany: implications of improving water quality. *Estuar Coast Shelf Sci* 107:112–121

Amann T, Weiss A, Hartmann J (2014) Silica fluxes in the inner Elbe Estuary, Germany. *Biogeochemistry* 118(1–3):389–412

Basile-Doelsch I (2006) Si stable isotopes in the Earth’s surface: a review. *J Geochem Explor* 88(1–3):252–256

Bergemann M, Blöcker G, Harms H, Kerner M, Meyer-Nehls R, Petersen W, Schroeder F (1996) Der Sauerstoffgehalt der Tideelbe. *Die Küste* 58:200–261

Beusen AHW, Bouwman AF, Dürr HH, Dekkers ALM, Hartmann J (2009) Global patterns of dissolved silica export to the coastal zone: results from a spatially explicit global model. *Glob Biogeochem Cycles* 23:1–13

Bianchi TS (2007) *Biogeochemistry of estuaries*. Oxford University Press, New York

Bidle KD (1999) Accelerated dissolution of diatom silica by marine bacterial assemblages. *Nature* 397(February):508–512

Bidle KD, Azam F (2001) Bacterial control of silicon regeneration from diatom detritus: significance of bacterial ectohydrolases and species identity. *Limnol Oceanogr* 46(7):1606–1623

BSH (2010) *Gezeitenkalender*. Bundesamt für Seeschifffahrt und Hydrographie, Hamburg

Carboneel V, Lionard M, Muylaert K, Chou L (2009) Dynamics of dissolved and biogenic silica in the freshwater reaches of a macrotidal estuary (The Scheldt, Belgium). *Biogeochemistry* 96(1–3):49–72

Cardinal D, Alleman LY, de Jong J, Ziegler K, Andre L (2003) Isotopic composition of silicon measured by multicollector plasma source mass spectrometry in dry plasma mode. *J Anal At Spectrom* 18(3):213–218

Cardinal D, Gaillardet J, Hughes HJ, Opfergelt S, André L (2010) Contrasting silicon isotope signatures in rivers from the Congo Basin and the specific behaviour of organic-rich waters. *Geophys Res Lett* 37(12):L12403

Conley DJ, Kilham SS, Theriot E (1989) Differences in silica content between marine and freshwater diatoms. *Limnol Oceanogr* 34(1):205–213

Dalrymple RW, Choi K (2007) Morphologic and facies trends through the fluvial–marine transition in tide-dominated depositional systems: a schematic framework for environmental and sequence-stratigraphic interpretation. *Earth Sci Rev* 81(3–4):135–174

De La Rocha CL, Bickle MJ (2005) Sensitivity of silicon isotopes to whole-ocean changes in the silica cycle. *Mar Geol* 217(3–4):267–282

De La Rocha CL, Brzezinski MA, Deniro MJ (1996) Purification, recovery, and laser-driven fluorination of silicon from dissolved and particulate silica for the measurement of natural stable isotope abundances. *Anal Chem* 68(21):3746–3750

De La Rocha CL, Brzezinski MA, DeNiro MJ (1997) Fractionation of silicon isotopes by marine diatoms during biogenic silica formation. *Geochim Cosmochim Acta* 61(23):5051–5056



- De La Rocha CL, Brzezinski MA, DeNiro MJ (2000) A first look at the distribution of the stable isotopes of silicon in natural waters. *Geochim Cosmochim Acta* 64(14):2467–2477
- De La Rocha CL, Bescont P, Croguennoc A, Ponzevera E (2011) The silicon isotopic composition of surface waters in the Atlantic and Indian sectors of the Southern Ocean. *Geochim Cosmochim Acta* 75(18):5283–5295
- Delstanche S, Opfergelt S, Cardinal D, Elsass F, André L, Delvaux B (2009) Silicon isotopic fractionation during adsorption of aqueous monosilicic acid onto iron oxide. *Geochim Cosmochim Acta* 73(4):923–934
- Delvaux C, Cardinal D, Carbonnel V, Chou L, Hughes HJ, André L (2013) Controls on riverine  $\delta^{30}\text{Si}$  signatures in a temperate watershed under high anthropogenic pressure (Scheldt—Belgium). *J Mar Syst* 128:40–51
- Demarest MS, Brzezinski MA, Beucher CP (2009) Fractionation of silicon isotopes during biogenic silica dissolution. *Geochim Cosmochim Acta* 73(19):5572–5583
- Ding T, Wan D, Wang C, Zhang F (2004) Silicon isotope compositions of dissolved silicon and suspended matter in the Yangtze River, China. *Geochim Cosmochim Acta* 68(2):205–216
- Ding TP, Ma GR, Shui MX, Wan DF, Li RH (2005) Silicon isotope study on rice plants from the Zhejiang province, China. *Chem Geol* 218(1–2):41–50
- Ding TP, Tian SH, Sun L, Wu LH, Zhou JX, Chen ZY (2008a) Silicon isotope fractionation between rice plants and nutrient solution and its significance to the study of the silicon cycle. *Geochim Cosmochim Acta* 72(23):5600–5615
- Ding TP, Zhou JX, Wan DF, Chen ZY, Wang CY, Zhang F (2008b) Silicon isotope fractionation in bamboo and its significance to the biogeochemical cycle of silicon. *Geochim Cosmochim Acta* 72(5):1381–1395
- Ding TP, Gao JF, Tian SH, Wang HB, Li M (2011) Silicon isotopic composition of dissolved silicon and suspended particulate matter in the Yellow River, China, with implications for the global silicon cycle. *Geochim Cosmochim Acta* 75(21):6672–6689
- Dürr HH, Meybeck M, Hartmann J, Laruelle GG, Roubeix V (2011) Global spatial distribution of natural riverine silica inputs to the coastal zone. *Biogeosciences* 8(3):597–620
- Ehlert C, Grasse P, Mollier-Vogel E, Boschen T, Franz J, de Souza GF, Reynolds BC, Stramma L, Frank M (2012) Factors controlling the silicon isotope distribution in waters and surface sediments of the Peruvian coastal upwelling. *Geochim Cosmochim Acta* 99:128–145
- Engström E, Rodushkin I, Baxter DC, Ohlander B (2006) Chromatographic purification for the determination of dissolved silicon isotopic compositions in natural waters by high-resolution multicollector inductively coupled plasma mass spectrometry. *Anal Chem* 78(1):250–257
- FGG Elbe (2012) Datenbank der Flussgebietsgemeinschaft Elbe (Dataset). Retrieved from <http://www.fgg-elbe.de>. Accessed 06 Dec 2012
- Fischer SM (1994) Untersuchungen zum Wasserhaushalt Tidebeeinflusster Vorlandmarschen im Ästuar der Elbe. In: Soil science. Universität Hamburg, Hamburger Bodenkundliche Arbeiten, Hamburg, p 209
- Fontorbe G, De La Rocha CL, Chapman HJ, Bickle MJ (2013) The silicon isotopic composition of the Ganges and its tributaries. *Earth Planet Sci Lett* 381:21–30
- Fraysse F, Pokrovsky OS, Schott J, Meunier J-D (2009) Surface chemistry and reactivity of plant phytoliths in aqueous solutions. *Chem Geol* 258(3–4):197–206
- Fripiat F, Cavagna AJ, Savoye N, Dehairs F, Andre L, Cardinal D (2011) Isotopic constraints on the Si-biogeochemical cycle of the Antarctic Zone in the Kerguelen area (KEOPS). *Mar Chem* 123(1–4):11–22
- Gardner LR (2005a) A modeling study of the dynamics of pore water seepage from intertidal marsh sediments. *Estuar Coast Shelf Sci* 62(4):691–698
- Gardner LR (2005b) Role of geomorphic and hydraulic parameters in governing pore water seepage from salt marsh sediments. *Water Resour Res* 41(7):W07010
- Georg RB, Reynolds BC, Frank M, Halliday AN (2006) Mechanisms controlling the silicon isotopic compositions of river waters. *Earth Planet Sci Lett* 249(3–4):290–306
- Georg RB, West AJ, Basu AR, Halliday AN (2009) Silicon fluxes and isotope composition of direct groundwater discharge into the Bay of Bengal and the effect on the global ocean silicon isotope budget. *Earth Planet Sci Lett* 283(1–4):67–74
- Goosen NK, Kromkamp J, Peene J, van Rijswijk P, van Breugel P (1999) Bacterial and phytoplankton production in the maximum turbidity zone of three European estuaries: the Elbe, Westerschelde and Gironde. *J Mar Syst* 22(2–3):151–171
- Grunwald M, Dellwig O, Kohlmeier C, Kowalski N, Beck M, Badewien TH, Kotzur S, Liebezeit G, Brumsack H-J (2010) Nutrient dynamics in a back barrier tidal basin of the Southern North Sea: time-series, model simulations, and budget estimates. *J Sea Res* 64(3):199–212
- Hartmann J, Jansen N, Dürr H, Harashima A, Okubo K, Kempe S (2010) Predicting riverine dissolved silica fluxes to coastal zones from a hyperactive region and analysis of their first-order controls. *Int J Earth Sci* 99(1):207–230
- Hiemstra T, Barnett MO, van Riemsdijk WH (2007) Interaction of silicic acid with goethite. *J Colloid Interface Sci* 310(1):8–17
- Hughes HJ, Bouillon S, Andre L, Cardinal D (2012) The effects of weathering variability and anthropogenic pressures upon silicon cycling in an intertropical watershed (Tana River, Kenya). *Chem Geol* 308:18–25
- Jones LHP, Handreck KA (1963) Effects of iron and aluminium oxides on silica in solution in soils. *Nature* 198(4883):852–853
- Kamatani A (1982) Dissolution rates of silica from diatoms decomposing at various temperatures. *Mar Biol* 68(1):91–96
- Kaufman PB, Dayanandan P, Takeoka Y, Bigelow WC, Jones JD, Iler R (1981) Silica in shoots of higher plants. In: Simpson TL, Volcani BE (eds) *Silicon and siliceous structures in biological systems*. Springer, New York, pp 409–449
- Kempe S (1992) Die Elbe, der geologische Blick. In: *Die Elbe - Ein Lebenslauf*. Deutsches Historisches Museum und Nicolai, Berlin, pp 25–33
- Kennett JP (1982) *Marine geology*. Prentice-Hall, Englewood Cliffs
- Kerner M (2007) Effects of deepening the Elbe Estuary on sediment regime and water quality. *Estuar Coast Shelf Sci* 75(4):492–500

- Loucaides S, van Cappellen P, Behrends T (2008) Dissolution of biogenic silica from land to ocean: role of salinity and pH. *Limnol Oceanogr* 53(4):1614–1621
- Manning BA, Goldberg S (1996) Modeling arsenate competitive adsorption on kaolinite, montmorillonite and illite. *Clay Clay Miner* 44(5):609–623
- Michalopoulos P, Aller RC (2004) Early diagenesis of biogenic silica in the Amazon Delta: alteration, authigenic clay formation, and storage. *Geochim Cosmochim Acta* 68(5):1061–1085
- Milligan AJ, Varela DE, Brzezinski MA, Morel FMM (2004) Dynamics of silicon metabolism and silicon isotopic discrimination in a marine diatom as a function of  $p\text{CO}_2$ . *Limnol Oceanogr* 49(2):322–329
- Mitsch WJ, Gosselink JG (1993) *Wetlands*. Wiley, New York
- Müller F, Struyf E, Hartmann J, Weiss A, Jensen K (2013) Impact of grazing management on silica export dynamics of Wadden Sea saltmarshes. *Estuar Coast Shelf Sci* 127:1–11
- Oelze M, von Blanckenburg F, Hoellen D, Dietzel M, Bouchez J (2014) Si stable isotope fractionation during adsorption and the competition between kinetic and equilibrium isotope fractionation: implications for weathering systems. *Chem Geol* 380:161–171
- Opfergelt S, Delmelle P (2012) Silicon isotopes and continental weathering processes: assessing controls on Si transfer to the ocean. *C R Geosci* 344(11–12):723–738
- Opfergelt S, Cardinal D, Henriot C, Draye X, André L, Delvaux B (2006) Silicon isotopic fractionation by banana (*Musa* spp.) grown in a continuous nutrient flow device. *Plant Soil* 285(1–2):333–345
- Opfergelt S, Eiriksdóttir ES, Burton KW, Einarsson A, Siebert C, Gislason SR, Halliday AN (2011) Quantifying the impact of freshwater diatom productivity on silicon isotopes and silicon fluxes: Lake Myvatn, Iceland. *Earth Planet Sci Lett* 305(1–2):73–82
- Pastuszak M, Conley DJ, Humborg C, Witek Z, Sitek S (2008) Silicon dynamics in the Oder Estuary, Baltic Sea. *J Mar Syst* 73(3–4):250–262
- Presti M, Michalopoulos P (2008) Estimating the contribution of the authigenic mineral component to the long-term reactive silica accumulation on the western shelf of the Mississippi River Delta. *Cont Shelf Res* 28(6):823–838
- Raven JA (2003) Cycling silicon—the role of Accumulation in Plants. *N Phytol* 158(3):419–421
- Reynolds BC, Frank M, Halliday AN (2006) Silicon isotope fractionation during nutrient utilization in the North Pacific. *Earth Planet Sci Lett* 244(1–2):431–443
- Schwedhelm E, Salomons W, Schoer J, Knauth H-D (1988) Provenance of the sediments and the suspended matter of the Elbe Estuary. In: GKSS 88/E/20. GKSS-Forschungszentrum Geesthacht GmbH, Geesthacht, p 76
- Sharp JH (2010) Estuarine oxygen dynamics: what can we learn about hypoxia from long-time records in the Delaware Estuary? *Limnol Oceanogr* 55:535–548
- Sharp JH, Culberson CH, Church TM (1982) The chemistry of the Delaware Estuary—general-considerations. *Limnol Oceanogr* 27(6):1015–1028
- Sicko-Goad LM, Schelske CL, Stoermer EF (1984) Estimation of intracellular carbon and silica content of diatoms from natural assemblages using morphometric techniques. *Limnol Oceanogr* 29(6):1170–1178
- Soetaert K, Middelburg J, Heip C, Meire P (2006) Long-term change in dissolved inorganic nutrients in the heterotrophic Scheldt Estuary (Belgium, The Netherlands). *Limnol Oceanogr* 51:409–423
- Strickland JD, Parsons TR (1972) *A practical handbook of seawater analysis*. Fisheries Research Board of Canada, Ottawa
- Struyf E, Conley DJ (2009) Silica: an essential nutrient in wetland biogeochemistry. *Front Ecol Environ* 7(2):88–94
- Struyf E, Conley DJ (2011) Emerging understanding of the ecosystem silica filter. *Biogeochemistry* 107(1–3):9–18
- Struyf E, van Damme S, Gribsholt B, Middelburg J, Meire P (2005) Biogenic silica in tidal freshwater marsh sediments and vegetation (Schelde Estuary, Belgium). *Mar Ecol Prog Ser* 303:51–60
- Struyf E, Temmerman S, Meire P (2006) Dynamics of biogenic Si in freshwater tidal marshes: Si regeneration and retention in marsh sediments (Scheldt Estuary). *Biogeochemistry* 82(1):41–53
- Struyf E, van Damme S, Gribsholt B, Bal K, Beauchard O, Middelburg JJ, Meire P (2007) *Phragmites australis* and silica cycling in tidal wetlands. *Aquat Bot* 87(2):134–140
- Struyf E, Smis A, Damme S, Meire P, Conley D (2009) The global biogeochemical silicon cycle. *Silicon* 1(4):207–213
- Sun X, Andersson PS, Humborg C, Pastuszak M, Mörth C-M (2013) Silicon isotope enrichment in diatoms during nutrient-limited blooms in a eutrophied river system. *J Geochem Explor* 132:173–180
- Sun X, Olofsson M, Andersson PS, Fry B, Legrand C, Humborg C, Mörth C-M (2014) Effects of growth and dissolution on the fractionation of silicon isotopes by estuarine diatoms. *Geochim Cosmochim Acta* 130:156–166
- Sutton JN, Varela DE, Brzezinski MA, Beucher CP (2013) Species-dependent silicon isotope fractionation by marine diatoms. *Geochim Cosmochim Acta* 104:300–309
- Tinsley D (1998) The Thames Estuary: a history of the impact of humans on the environment and a description of the current approach to environmental management. In: Attrill MJ (ed) *A rehabilitated estuarine ecosystem: the environment and ecology of the Thames Estuary*. Kluwer Academic Publishers, Dordrecht, pp 5–26
- Tréguer PJ, De La Rocha CL (2013) The world ocean silica cycle. *Annu Rev Mar Sci* 5(1):477–501
- Tréguer P, Nelson DM, van Bennekom AJ, DeMaster DJ, Leynaert A, Quéguiner B (1995) The silica balance in the world ocean: a reestimate. *Science* 268(5209):375–379
- UVU (1997) *Umweltverträglichkeitsuntersuchung Zur Anpassung der Fahrrinne der Unter- und Aussenelbe an die Containerschifffahrt*. Wasser- und Schifffahrtsamt, Hamburg
- Varela DE, Pride CJ, Brzezinski MA (2004) Biological fractionation of silicon isotopes in Southern Ocean surface waters. *Glob Biogeochem Cycles* 18(1):GB1047
- Vieillard AM, Fulweiler RW, Hughes ZJ, Carey JC (2011) The ebb and flood of Silica: quantifying dissolved and biogenic silica fluxes from a temperate salt marsh. *Estuar Coast Shelf Sci* 95(4):415–423
- Weiss JV, Emerson D, Magonigal JP (2004) Geochemical control of microbial Fe(III) reduction potential in wetlands: comparison of the rhizosphere to non-rhizosphere soil. *FEMS Microbiol Ecol* 48(1):89–100

- Weiss A, Amann T, Hartmann J (2012) Silica dynamics of tidal marshes in the Inner Elbe Estuary, Germany. *Silicon* 5(1):75–89
- Weiss A, Amann T, Hartmann J (2013) Silica dynamics of tidal marshes in the Inner Elbe Estuary, Germany. *Silicon* 5(1):75–89
- Wetzel F, de Souza GF, Reynolds BC (2014) What controls silicon isotope fractionation during dissolution of diatom opal? *Geochim Cosmochim Acta* 131:128–137
- Wolfstein K, Kies L (1995) A case study on the oxygen budget in the freshwater part of the Elbe Estuary. 3. Variations in phytoplankton pigments in the Elbe before and during the oxygen minima in 1992 and 1993. *Arch Hydrobiol (Suppl)* 110(1):39–54
- Yamada SS, D'Elia CF (1984) Silicic-acid regeneration from estuarine sediment cores. *Mar Ecol Prog Ser* 18(1–2):113–118
- Ziegler K, Chadwick OA, Brzezinski MA, Kelly EF (2005) Natural variations of  $\delta^{30}\text{Si}$  ratios during progressive basalt weathering, Hawaiian Islands. *Geochim Cosmochim Acta* 69(19):4597–4610